Progress In Electromagnetics Research M, Vol. 80, 169–179, 2019

Vertical Polarized 1×3 Series-Fed Linear Array with Gain and Front-to-Back Ratio Enhancement for Airborne SAR-X Applications

Venkata Kishore Kothapudi* **and Vijay Kumar**

Abstract—In this paper, a gain and front-to-back ratio (FTBR) enhanced vertically polarized 1×3 series-fed linear array for Airborne Synthetic Aperture Radar-X-band applications has been presented. The proposed antenna prototype is designed at 9.65 GHz (X-band). The design consists of a square radiating patch, substrate, quarter wave transformer, 50 Ω matched transformer, and series feed line (SFL). The simulated antenna prototype is fabricated and successfully measured. The final antenna prototype has a dimension $3.256 \times 2.035 \times 0.0645\lambda_g^3$ (Guided wavelength) at 9.65 GHz. The results indicate that the proposed antenna prototype yields an impedance bandwidth $>$ 140 MHz (from 9.591 to 9.712 GHz) defined by $S11 < -10$ dB. The low profile/cost antenna prototype has a fully directional radiation pattern with measured gain up to 12.2 dBi and estimated radiation efficiency of 89%, respectively. A brass plate with 0.8 mm thickness has been fabricated to attach to the antenna ground plane for improving FTBR of more than 30 dB. All these features make the proposed antenna array have good potential applications in X-band system, especially in 9.65 GHz Airborne SAR systems. The aperture of the antenna is 80 mm × 50 mm, which equals 31 wavelengths at 9.65 GHz.

1. INTRODUCTION

X-band SAR is specifically suited for reconnaissance and disaster monitoring, providing the best spatial resolution, thus best suited for surveillance. SAR antennae are usually bulky, heavy, and expensive in SAR systems (Skolnik, 1970) [1]. Compared with the systems using L-, S-, C-bands, X-band systems have the advantages of compactness, flexibility, and manoeuvrability (Imbriale et al., 2012) [2]. Several factors that degrade radar performance are caused by the antennas used; these factors are front-to-back ratio, side-lobe level, co-polarization, cross-polarization, and half power beam width (HPBW). For example, the signals transmitted from an antenna can radiate scatters through the side lobes or back lobe, and the returned echoes are received in the same manner in receiving mode. The unwanted signals falsely display a target in the main-beam direction, thereby causing the error to be detected. Microstrip antenna arrays are widely used in numerous wireless communication applications such as radar and satellite systems, since they usually have low profile, low cost, light weight, and high gain. (Lee et al., 2001; Barba, 2008; Hajian et al., 2009; Hautcoeur et al., 2010; Huque et al., 2011; Iizukat et al., 2003; Jung et al., 2012; Li et al., 2012) [3–10].

An X-band directive single microstrip patch antenna to vary the beam width of the patch from 18 to 125 deg has been proposed with proper choice of parasite parameters and proposed by (Afzalzadeh and Karekar, 1992) [11]. Alumina sheets were used as superstrates of two different sizes as dielectric parasites with a gain of 10 dBi by (Andrenko et al., 2006) [12]. It has an SLL of −15 dB and a cross-pol of −25 dB. Microstrip-fed dielectric resonator antennas for X-band applications have been proposed by

Received 12 December 2018, Accepted 14 March 2019, Scheduled 18 April 2019
* Corresponding author: Venkata Kishore Kothapudi (v.k.kothapudi@ieee.org).
The authors are with the Department of Communication Engineering, School of Electronics Engineering, Vellore Institute of Technology (VIT), Vellore, Tamilnadu 632014, India.

(Coulibaly et al., 2008) [13] at the center frequency of 10 GHz with a size of 30.08 mm × 45.9 mm. A probe-fed rectangular microstrip antenna for X-band applications was presented in [14] by (Verma and Shrivastava, 2011), but this was only for a single resonance frequency (9 GHz). For X-band applications, an S-shaped patch antenna was designed with two slots to perturb the surface current path at resonant frequency with −41 dB return loss and gain of 6 dBi at 10 GHz by (Aggarwal and Garg, 2012) [15] which was half the gain of the work presented in this research. A broadband antenna operating in X-band applications with 5.1 dBi gain was presented by (Harrabi et al., 2013) [16]. The antenna is made of a polygon with a circular slot and a Teflon layer (Radom), which increases the performance of the antenna. An X-band woodpile electromagnetic bandgap (EBG) material has been designed by (Frezza et al., 2014) [17] for the planar antenna to achieve high gain, which is complex in design and fabrication compared to the study proposed in this article.

In the literature review above, it can be easily concluded that the previously proposed designs have either high design complexity and low gain or are costly. Recently authors reported X-band 1×2 linear array design with direct coupling at 9.3 GHz centre frequency having a gain of 10.6 dBi with series feeding method in both XZ- and YZ-planes by (Kothapudi and Kumar, 2017) in [18]. A 1×2 linear array design at 9.65 GHz with 10 dBi gain having a size of $60 \times 40 \times 0.8\,\text{mm}^3$ has been proposed by authors (Kothapudi and Kumar, 2018) in [19], and the present work provides 2 dB higher gain than the work presented in [18, 19]. The bandwidth of the antenna design can be greatly increased through the use of the metamaterials, reaching a bandwidth of 10.8 GHz with high gain implemented with a voltage standing wave ratio (VSWR) that remains below 2.0 : 1, and the design has dimensions of $30.6 \times 35.3 \times 0.8\,\text{mm}^3$. Wave propagation along the patch induces the strongest radiation in horizontal direction, rather than in the vertical direction of a conventional patch antenna by (Xu et al., 2013) in [20]. Metamaterial Transmission lines (MTM TLs) which feature dual-shunt branches in the circuit model have been thoroughly investigated for multi frequency monopoles. The CMTLs can be easily integrated with the planar monopoles in which the ground plane remains unaltered [21].

In this paper, a low-cost low-profile single-port 1×3 series-fed linear array antenna using direct coupling with quarter wave transformer is presented. The proposed antenna prototype is designed at 9.65 GHz X-band. The substrate thickness of 0.787 mm (31 mil) with 1 oz. copper cladding makes the prototype feasible. The process of design and parametric studies are illustrated in detail. The final antenna prototype has dimensions of $80 \times 50 \times 1.587\,\text{mm}^3$ at 9.65 GHz. From the radiation pattern it is observed that FTBR is more than 30 dB, HPBW 69.8° in E-plane and 21.6° in H-plane, respectively, is obtained. The side lobe level (SLL) is more than −22.9 dB and −10.6 dB in E-plane and H-plane, respectively. The X-pol levels are −30 dB in both E-plane and H-plane. The antenna prototypes are analyzed by performing full wave simulation using an industry standard FIT based CST MWS software 2016. The antenna has been fabricated and tested. The measured results agree well with the simulated ones. The proposed antenna structure and design are discussed in Section 2, and parametric analysis and results of prototype are discussed in Sections 3 and 4. Finally, the conclusions are drawn in Section 5.

2. ANTENNA STRUCTURE AND DESIGN

The proposed antenna configuration and the 1×3 linear array antenna with one excitation port as a unit cell of the arrays are designed at 9.65 GHz. This 9.65 GHz, 1×3 linear array consists of a microstrip line feeding or direct coupling to match the antenna impedance and series feeding for array at the top layer, and a ground plane at the bottom layer. The square array geometry with patch elements with series feed line can reduce the antenna losses. In this work, an RT/Duroid 5880 (made by Rogers) copper cladding substrate with 31 mil (0.787 mm) height, 1 Oz, i.e., 0.035 mm thick copper Rogers relative permittivity $\varepsilon_r = 2.2$ and loss tangent $\tan d = 0.0009$ is chosen as the antenna material [22]. All the metal components in the reported antenna design are taken to be copper with its known material parameters $\varepsilon_r = 1$, $\mu_r = 1$, and bulk conductivity $\sigma = 5.8 \times 10^7$ s/m. The feed line and patches were patterned or etched on the top cladding layer with the laser milling machine whereas the bottom cladding layer acts as the ground plane. After fabrication of the antenna, we went through gold plating on the top and bottom of the copper layer of 1-micron thickness for better conductivity. Later antenna mounting plate with a brass material of 0.8 mm thickness was fabricated which was used to mount the antenna PCB using M2 (M-Metric Standard) Stainless Steel screws. Gold plated Amphenol RF Subminiature-A

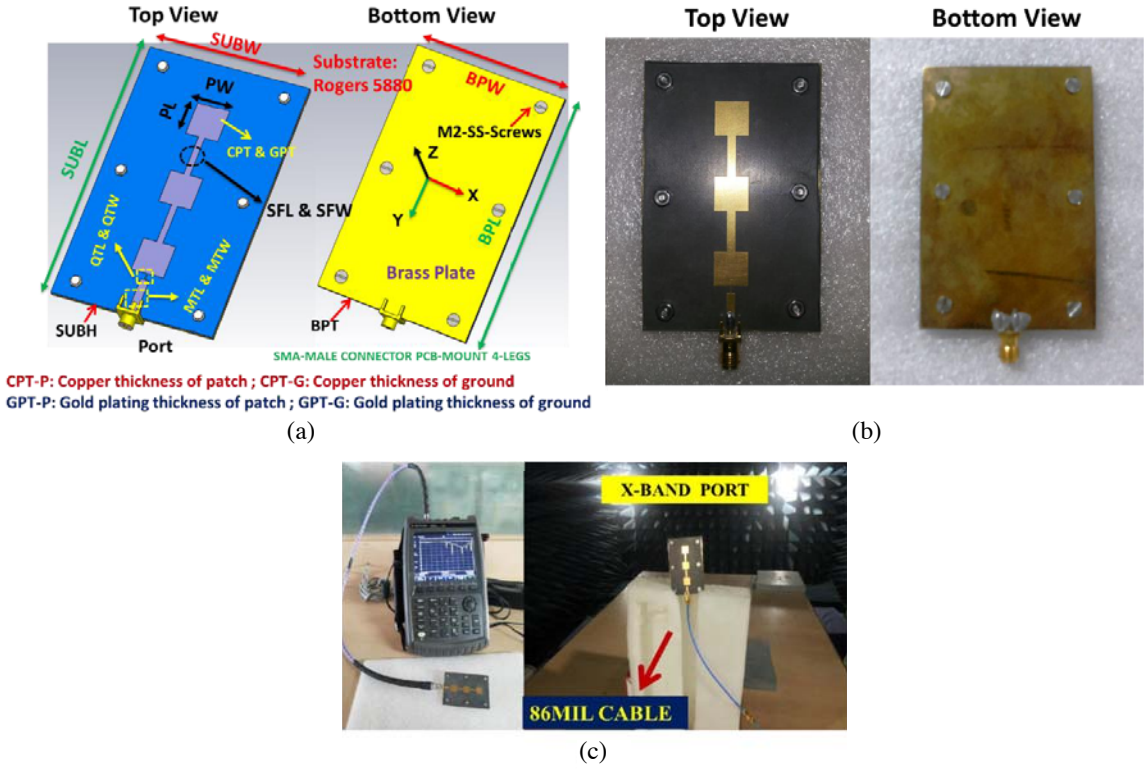

Figure 1. Geometry of the proposed antenna prototype with overall dimension of $80 \times 50 \times 1.587\,\text{mm}^3$. (a) Top and Bottom view of CST model with dimensions. (b) Fabricated prototype top and bottom view. (c) X-band measurement setup — S-parameters with VNA and Radiation pattern measurement.

(SMA) male extended legs (Part no: 132134) connector was used to solder the microstrip line feed. All simulations are performed using CST Microwave Studio 2016 [23], an industry standard software simulator based on FIT-Finite Integration Technique that is equivalent to FDTD-Finite Difference Time Domain.

Figure 1 shows the geometry configuration of the 1×3 series-fed linear array with single RF antenna port. S_{11} shows the best case QTW = 0.28; QTL = 2 ($\lambda_g = 24.57$; $\lambda_g/4 = 6.14$ with optimization for a resonant frequency of 9.65 GHz, and the value of quarter-wave transformer is 2 mm which is approximately $\lambda_g/10$) and QTW = 0.2 mm ($\approx 146\,\Omega$). This impedance variation is because of array environment. The effect of series feeding leads to impedance change in quarter wave transformer ($\lambda_g/4$). The patches are connected to each other by series feeding using the lines with dimensions of SFW and SFL which are 1.9 mm and 20 mm from the patch feed point to patch feed point towards Y-direction. To design a 0.7λ array, the value of SFL was selected to be 20 mm which provides a scan angle of $\pm 25°$ in the elevation plane from zenith angle of the upper hemisphere based on Equation (1). To improve the impedance matching between the elements, the value of SFW was selected and optimized to 1.9 mm ($\approx 59\,\Omega$).

The optimization was done so that the array would have the maximum gain and good matching at phi = 0 and theta = 0. The S parameters of the optimized array are presented in Figure 5 and show a good matching around 9.56 GHz to 9.7 GHz (140 MHz, 1.4%). By using the simulation software CST, simulated surface current distribution, magnitude of E-fields, and a magnitude of H-fields in the microstrip line feed and radiating patch for the cases with QTL, QTW, MTL, and MTW were obtained at resonant frequency 9.65 GHz and shown in Figures 2(a)–(c). The designed antenna prototype's Smith chart, impedance parameters (Z-parameters) (real and imaginary), and phase angle of S_{11} are calculated using CST MWS-2016 and shown in Figures 3(a)–(c). A better impedance matching has been observed in the targeted 9.65 GHz resonant frequency by achieving the real part 48.5 Ω while the

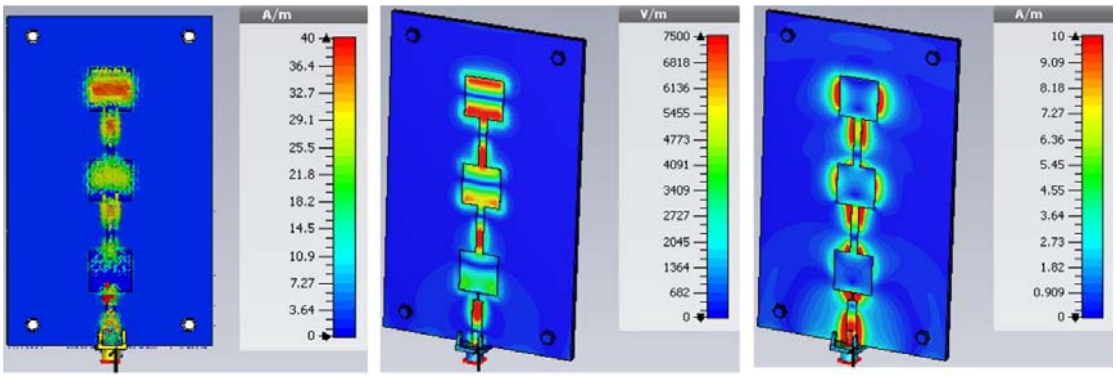

(a) (b) (c)

Figure 2. Simulated (a) surface current distribution. (b) Magnitude of E-field, and (c) magnitude of H-field in the direct coupled feedline and radiating patch of the antenna prototype — 1×3.

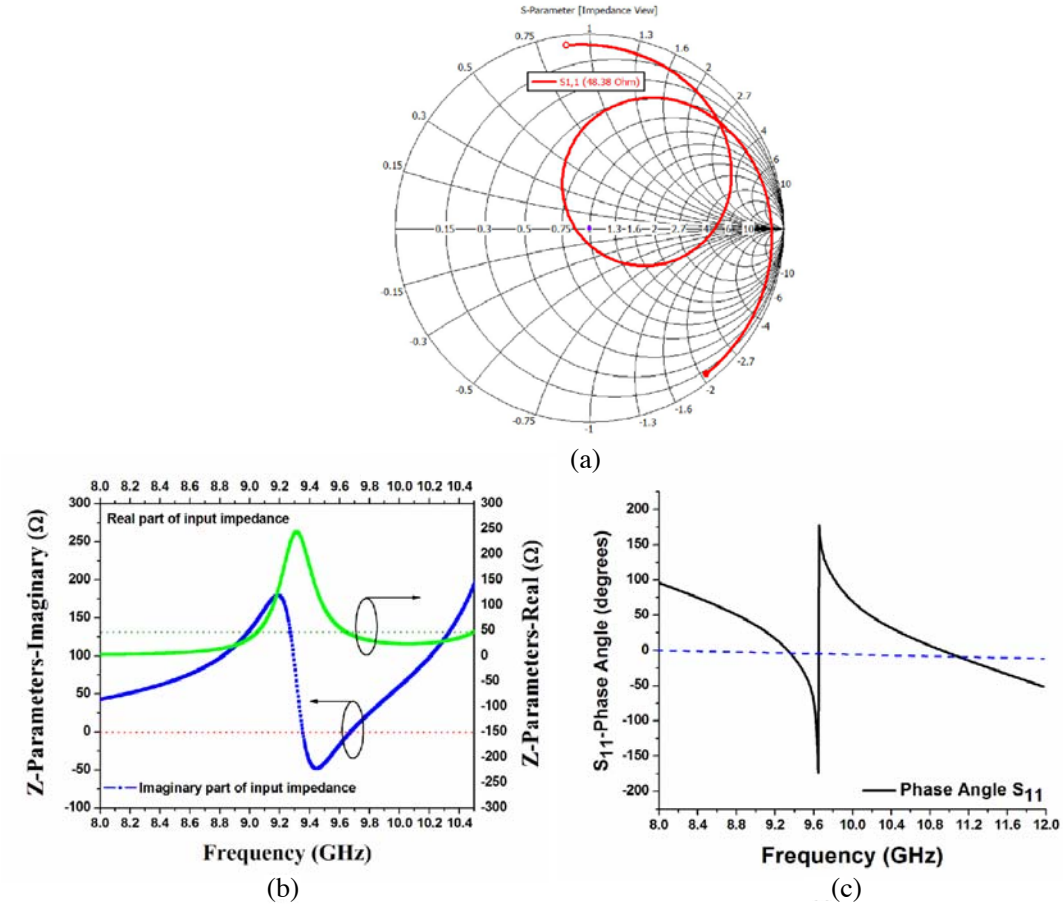

(a) (b) (c)

Figure 3. Simulated (a) Smith chart (48.5 Ω), (b) Z-parameters Real and Imaginary part. (c) Phase angle of S_{11}.

imaginary part gets closer to 0 Ω as a result better impedance matching over the operating band. The optimized dimensions of prototype are given in Table 1.

$$d_y = \frac{\lambda_V}{1 + \sin\theta_y} \tag{1}$$

d_y = Inter-element spacing between the elements in y-direction

Table 1. Optimized dimensions of the antenna design prototype of 1×3 linear array.

Parameter	Description	Value (mm)	Value (λ_0)	Value (λ_g)
PL	Length of the patch	10	0.3217	0.407
PW	Width of the patch	10	0.3217	0.407
QTL	Length of the quarter wave transformer	2	0.0643	0.0814
QTW	Width of the quarter wave transformer	0.28	0.009	0.01139
MTL	Length of the matching transformer	10.25	0.3287	0.4171
MTW	Width of the matching transformer	2.46	0.0791	0.100
SFL	Length of the series-fed line	22	0.7078	0.8954
SFW	Width of the series-fed line	1.9	0.0611	0.0773
SUBL	Length of the substrate	80	2.574	3.256
SUBW	Width of the substrate	50	1.6087	2.035
SUBH	Height of the substrate	0.787	0.0253	0.03203
BPL	Length of the brass plate	80	2.574	3.256
BPW	Width of the brass plate	50	1.6087	2.035
BPT	Thickness of the brass plate	0.8	0.02574	0.03256
CPT-P	Thickness of the copper-patch	0.035	0.001126	0.001424
CPT-G	Thickness of the copper-ground	0.035	0.001126	0.001424
GPT-P	Gold plating thickness-patch	0.001	0.00003217	0.0000407
GPT-G	Gold plating thickness-ground	0.001	0.00003217	0.0000407

λ = Free space wavelength at 9.65 GHz
λ_V = Free space wavelength in V-port
θ = Maximum scan angle

3. PARAMETRIC ANALYSIS

The results of the parametric studies on the proposed prototype are presented and shown in Figures 4(a)–(e). The parameters considered are QTL, QTW, MTL, MTW, SFL, and SFW. The simulation results for how the antennas performance in terms of S_{11} affected by varying each parameter are provided. A tested example, with geometrical dimensions of QTL = 4 mm, QTW = 0.28 mm, MTL = 10.25 mm, MTW = 2.46 mm, SFL = 22 mm, and SFW = 1.9 mm, is selected to demonstrate the impedance matching performance of the proposed prototype. To understand the effects of varying QTL, QTW, MTL, and MTW on the antenna performance, a parametric analysis is performed. Only one parameter is investigated at a time, and the other dimensions are the same as those of the example. The simulation results are discussed to provide knowledge on how the antenna's performance in terms of S_{11} is affected by varying each parameter.

3.1. Varying QTL

Figure 4(a) demonstrates the performance of the proposed prototype antenna when the QTL of the top and bottom of the length is varied. By varying the QTL from 3 mm to 5 mm with a step size of 0.2 mm in the present design, there is a shift towards the lower frequencies when QTL is 5 mm and shift towards higher frequency when QTL is 3 mm. Good impedance matching is obtained at 4 mm, for fixed values of QTW, MTL, SFL, SFW, and MTW. From the results obtained, it is seen that the operating frequency at 9.65 GHz is excited with good matching conditions. In order to cover the operating frequency bands of X-band range 9.5–9.7 GHz, the QTL value is set to 4 mm.

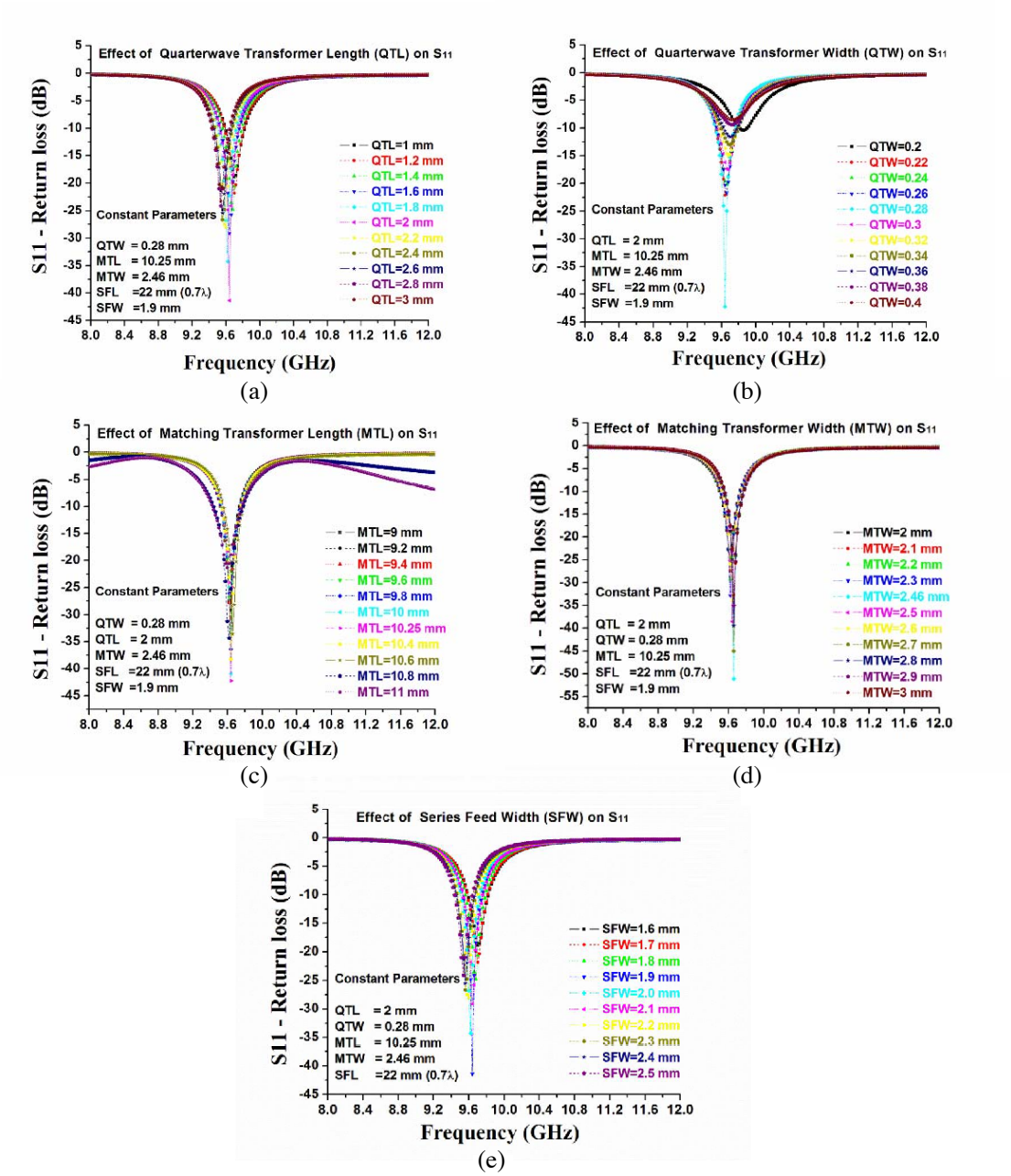

Figure 4. Simulated parametric analysis. (a) Effect of QTL on S_{11}. (b) Effect of QTW on S_{11}. (c) Effect of MTL on S_{11}. (d) Effect of MTW on S_{11} and (e) Effect of SFW on S_{11}.

3.2. Varying QTW

Figure 4(b) demonstrates the performance of the proposed prototype antenna when the quarter wave transformer width (QTW) of the left and right of the width is varied from center position. By varying the QTW from 0.2 mm to 0.4 mm with a step size of 0.02 mm in the present design, there is a more reflection observed when QTW is 0.2 mm, and QTW is 0.4 mm. In the case of 0.2 mm shift in frequency towards higher band, more reflection has been observed. Good impedance matching is obtained at 0.28 mm, for fixed values of QTL, MTL, SFL, SFW, and MTW. From the results obtained, it is seen that the operating frequency at 9.65 GHz is excited with good matching conditions. The reason may be results from the increase of the reactance caused by the loading effect. In order to cover the operating frequency bands of the X-band range 9.5–9.7 GHz, the QTW value is set to 0.28 mm.

3.3. Varying MTL

Figure 4(c) demonstrates the performance of the proposed prototype antenna when the MTL of the top and bottom of the length is varied. By varying the MTL from 9 mm to 11 mm with a step size of 0.2 mm in the present design, there is a variation in the impedance matching. Good impedance matching is obtained at 10.25 mm, for fixed values of QTW, QTL, SFL, SFW, and MTW. From the results obtained, it is seen that the operating frequency at 9.65 GHz is excited with good matching conditions. In order to cover the operating frequency bands of the X-band range 9.5–9.7 GHz, the MTL value is set to 10.25 mm.

3.4. Varying MTW

Figure 4(d) demonstrates the performance of the proposed prototype antenna when the matching transformer width (MTW) is varied from center position. By varying the MTW from 2 mm to 3 mm with a step size of 0.1 mm in the present design, there is a good impedance matching obtained at 2.46 mm, for fixed values of QTL, MTL, SFL, SFW, and QTW. From the results obtained, it is seen that the operating frequency at 9.65 GHz is excited with good matching conditions. In order to cover the operating frequency bands of the X-band range 9.5–9.7 GHz, the MTW value is set to 4 mm.

3.5. Varying SFW

Figure 4(e) demonstrates the performance of the proposed prototype antenna when the series-feed width (SFW) is varied from center position. By varying the SFW from 1.6 mm to 2.5 mm with a step size of 0.1 mm in the present design, there is a good impedance matching obtained at 1.9 mm, for fixed values of QTL, QTW, MTL, SFL, and MTW. From the results obtained, it is seen that the operating frequency at 9.65 GHz is excited with good matching conditions. In order to cover the operating frequency bands of the X-band range 9.5–9.7 GHz, the MTW value is set to 1.9 mm.

4. SIMULATED AND EXPERIMENTAL RESULTS AND ANALYSIS

The X-band series-fed 1×3 linear array prototype with its center frequency of 9.65 GHz has been fabricated and measured to validate the design. The fabricated prototype with top and bottom views is shown in Figure 1(b). The simulated and measured results are given for X-band. The S-parameters and radiation patterns are measured using Agilent N9918A field fox microwave analyzer, and the radiation patterns and gain measurements were measured in an anechoic chamber (supplier: Haining ocean import and export Co. Ltd) of $6\,\text{m} \times 4\,\text{m} \times 3\,\text{m}$ ($L \times W \times H$) with Agilent PNA series network analyzer N5230C (10 MHz to 40 GHz). The measurement setups for both S-parameters and radiation pattern are shown in

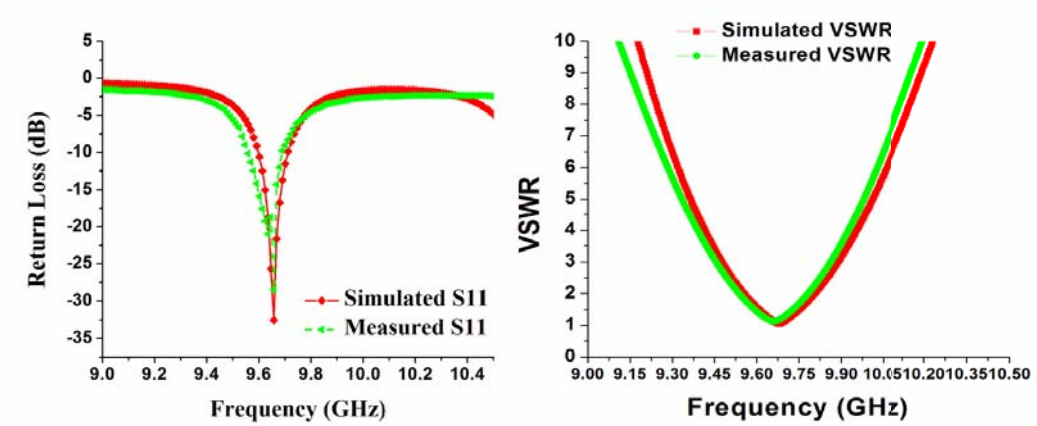

Figure 5. Simulated and measured S-parameters for the prototype — 1×3. (a) Return loss. (b) VSWR.

Figure 1(c). The simulated and measured input S_{11} characteristics of the proposed 1×3 series-fed linear array are compared in Figure 5(a), and voltage standing wave ratio (VSWR) is given as Figure 5(b). A measured impedance bandwidth of 1.46% (9.588–9.701 GHz) is obtained with respect to simulated values of (9.591–9.712 GHz).

The radiation pattern is measured in an anechoic chamber using a double-ridge horn antenna as the reference antenna having gain (Gr) of 10 dBi at X-band. The reference antenna and proposed antenna are kept at a distance (R) of 300 cm. The power received by the horn antenna was -30.98 dBm, and the power received by the antenna under test (AUT) was around -28.69 dBm. The transmitted power (Pt) is 0 dBm. The received power (Pr) is -30.89 dBm at X-band. The gain of the antenna under test (Gt) is calculated using Friis transmission equation as follows:

$$P_r = P_t G_t G_r \left(\frac{\lambda^2}{4\pi R}\right) \tag{2}$$

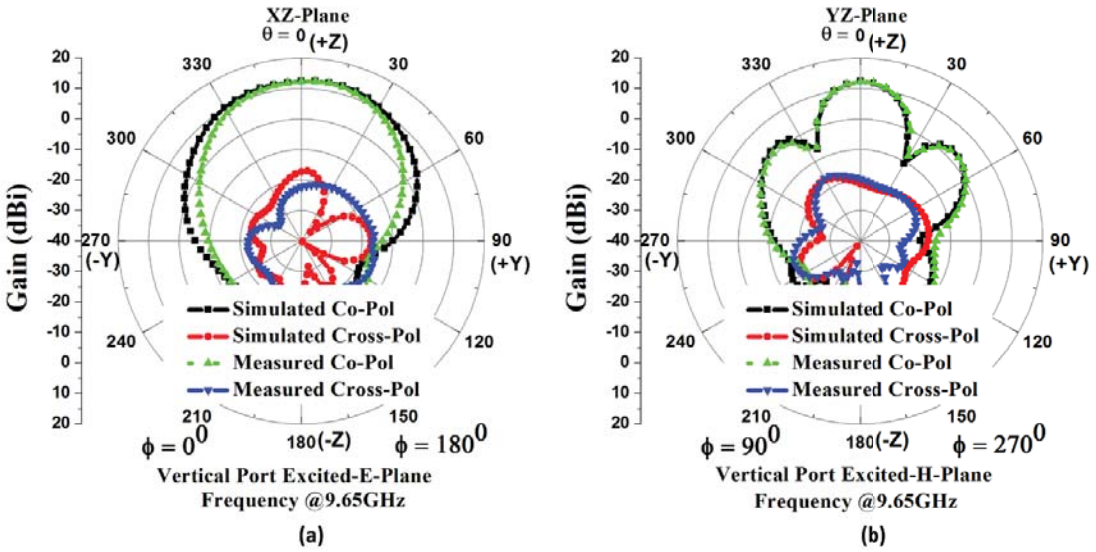

Figure 6. Simulated and measured E-plane (XZ-Plane) — co-pol and cross-pol and H-plane (YZ-Plane) — co-pol and cross-pol radiation patterns at resonant frequency 9.65 GHz. (a) E-Plane. (b) H-Plane for the antenna prototype — 1×3.

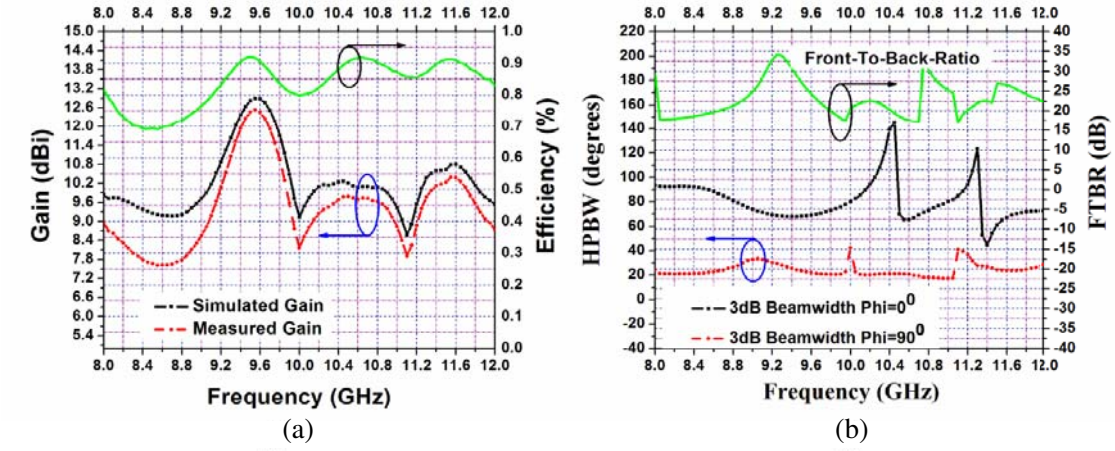

Figure 7. (a) Simulated and measured gain and simulated efficiency against the frequency of the antenna prototype. (b) Half power beam width and front-to-back-ratio over the frequency for 1×3 linear array.

The measured and simulated radiation patterns in terms of E-plane and H-plane 2D polar plots are shown in Figures 6(a) and (b). Exciting RF antenna port, it is observed that the E-plane with co-pol and cross-pol components has a main lobe magnitude of 12.1 dBi, side lobe level of −25.1 dB, front to back ratio (FTBR) of 32.83 dB, and an angular half power beam width (HPBW) of 78.4, respectively. In contrast, the H-plane with its co-pol and cross-pol components has a main lobe magnitude of 12.2 dBi, side lobe level of −10.5 dB, FTBR of 32 dB, and an HPBW of 25, respectively. The measured gain and efficiency of the proposed antenna are shown in Figure 7(a). At the center frequency, RF antenna port achieves a gain of 12.2 dBi. The simulated antenna efficiency is above 89% over the impedance bandwidth. Figure 7(b) shows the FTBR and HPBW over frequency, which shows that there is a good agreement over impedance bandwidth. Figures 8(a) and (b) show 3D radiation patterns of the proposed antenna for E- and H-planes. When RF antenna port is excited, the antenna achieves a gain of 12.2 dBi. The antenna performance characteristics such as side lobe level (SLL), front-to-back ratio (FTBR), gain, 3 dB beamwidth (HPBW), efficiency, and cross-polarization (X-pol) level are calculated and summarized in Table 2. The measured results mostly agree and reflect the results produced via simulations. Comparison with existing literature has been provided in Table 3.

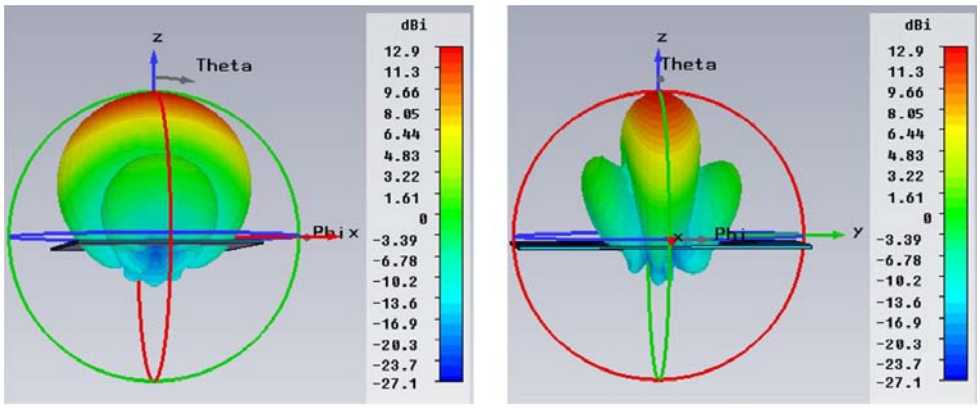

Figure 8. Simulated far-field gain at 9.65 GHz for 1 × 3 linear array (a) E-Plane (b) H-Plane.

Table 2. Performance analysis of the antenna prototype of 1 × 3 linear array.

Parameter		**1 × 3 Linear Array**	
		Simulated	**Measured**
Band width (GHz)		9.591–9.712	9.588–9.701
Gain		12.1	12.2
Radiation efficiency		91.1	89.04
E-Plane	SLL (dB)	−25.1	−22.9
	HPBW (deg)	78.4	69.8
	Cross-pol (dB)	−31	−30
	FTBR (dB)	32.83	31
H-Plane	SLL (dB)	−10.5	−10.6
	HPBW (deg)	24	21.6
	Cross-pol (dB)	−28	−30
	FTBR (dB)	32	31
Aperture area (Ap)		4000 mm^2	
Effective area (Ae)		664 mm^2	
Aperture efficiency (ea)		16.6%	

Table 3. Comparison with existing literature.

Article	Year	Element	Size	Resonant frequency (GHz)	Gain (dBi)	Application	Software tool
Ref. [11]	1992	Patch	$25.4 \times 25.4 \times 0.635\,\text{mm}^3$	9.76	N/A	X-band	N/A
Ref. [12]	2006	Circular patch	N/A	8.65	10	X-band	N/A
Ref. [13]	2008	Microstrip-fed stepped patch DRA	N/A	10	N/A	X-band	CST
Ref. [14]	2011	Rectangular patch	$10.1 \times 13.9 \times 1.6\,\text{mm}^3$	9	8.57	X-band	CST
Ref. [15]	2012	S-shaped patch	$45.9 \times 30.08 \times 1.3\,\text{mm}^3$	10	6	X-band	HFSS
Ref. [16]	2013	Patch	$7.56 \times 18.04 \times 1.6\,\text{mm}^3$	9.75	5.1	X-band	CST
Ref. [17]	2014	Woodpile EBG	NA	10.3	18	X-band	HFSS
This work	1×3	Square patch 1×3 linear array antenna with brass plate	$80 \times 50 \times 1.587\,\text{mm}^3$	9.65	12.2	X-band	CST

5. CONCLUSION

A gain and front-to- back ratio enhancement vertical polarized 1×3 series-fed linear array for airborne SAR-X applications has been designed and fabricated. By using a series-fed network, the losses associated with feed line becomes less. Its radiation characteristics can be improved by using a series-fed structure as a feeding network. The antenna prototype has dimension of $80 \times 50 \times 1.587\,\text{mm}^3$ or $2.574 \times 1.6087 \times 0.051\lambda_0^3$ (Free space wavelength) or $3.256 \times 2.035 \times 0.0645\lambda_g^3$ (Guided wavelength) at 9.65 GHz. The antenna prototypes have been fabricated and experimentally characterized. The good agreement between simulated and experimental results has validated the design. In addition, the antenna provides stable radiation patterns, 3 dB beamwidth, SLL, and good FTBR for SAR applications. Moreover, the proposed prototype antennas also feature simple and compact structures. The S-parameters and radiation parameters are discussed. The antenna gain and efficiency are also given. A brass plate has been introduced in ground plane to improve the front to back ratio (FTBR) around 30 dB. The antenna has advantages of easy fabrication, assembling, and low profile. A detailed comparison between simulated and measured results of the proposed 1×3 linear array is also presented.

ACKNOWLEDGMENT

The work has been done at Microwave division, School of Electronics engineering (SENSE), VIT University, Vellore, Tamil nadu, India. All the assistance provided by the department and university administration to carry out this work is highly appreciated. The authors express their thanks to reviewers of this manuscript.

REFERENCES

1. Skolnik, M. I., *Radar Handbook*, McGraw-Hill, New York, NY, USA, 1970.
2. Imbriale, W. A., S. Gao, and L. Boccia, Eds., *Space Antenna Handbook*, Wiley, New York, NY, USA, 2012.
3. Jung, Y.-B., I. Yeom, and C. W. Jung, "Centre-fed series array antenna for k-/ka-band electromagnetic sensors," *IET Microw. Antennas Propag.*, Vol. 6, No. 5, 588–593, Apr. 2012.

4. Hajian, M., J. Zijderveld, A. A. Lestari, and L. P. Ligthart, "Analysis, design and measurement of a series-fed microstrip array antenna for X-band INDRA: The Indonesian maritime radar," *Proc. 3rd Eur. Conf. Antennas Propag.*, 1154–1157, Berlin, Germany, Apr. 2009.
5. Huque, T., K. Hossain, S. Islam, and A. Chowdhury, "Design and performance analysis of microstrip array antennas with optimum parameters for X-band applications," *Int. J. Adv. Comput. Sci. Applicat.*, Vol. 2, No. 4, 81–87, 2011.
6. Hautcoeur, J., E. M. Cruz, J. Bartholomew, J. Sarrazin, Y. Mahe, and S. Toutain, "Low-cost printed antenna array built with hybrid feed for urban microwave links," *IET Microw. Antennas Propag.*, Vol. 4, No. 9, 1320–1326, Sep. 2010.
7. Iizuka, H., K. Sakakibara, T. Watanabe, K. Sato, and K. Nishikawa, "Millimeter-wave microstrip array antenna with high efficiency for automotive radar systems," *R&D Rev. Toyota CRDL*, Vol. 37, No. 2, 7–12, 2002.
8. Barba, M., "A high-isolation, wideband and dual-linear polarization patch antenna," *IEEE Trans. Antennas Propag.*, Vol. 56, No. 5, 1472–1476, May 2008.
9. Lee, B., S. Kwon, and J. Choi, "Polarization diversity microstrip base station antenna at 2 GHz using t-shaped aperture-coupled feeds," *IEE Proc. Microw. Antennas Propag.*, Vol. 148, No. 5, 334–338, Oct. 2001.
10. Li, B., Y.-Z. Yin, W. Hu, Y. Ding, and Y. Zhao, "Wideband dual-polarized patch antenna with low cross polarization and high isolation," *IEEE Antennas Wireless Propag. Lett.*, Vol. 11, 427–430, Apr. 2012.
11. Afzalzadeh, R. and R. N. Karekar, "X-band directive single microstrip patch antenna using dielectric parasite," *Electronics Letters*, Vol. 28, No. 1, 17–19, 1992.
12. Andrenko, A. S., I. V. Ivanchenko, D. I. Ivanchenko, et al., "Active broad X-band circular patch antenna," *IEEE Antennas and Wireless Propagation Letters*, Vol. 5, No. 1, 529–533, 2006.
13. Coulibaly, Y., T. A. Denidni, and H. Boutayeb, "Broadband microstrip-fed dielectric resonator antenna for X-band applications," *IEEE Antennas and Wireless Propagation Letters*, Vol. 7, 341–345, 2008.
14. Verma, A. and N. Srivastava, "Analysis and design of rectangular microstrip antenna in X band," *MIT International Journal of Electronics and Communication Engineering*, Vol. 1, No. 1, 31–35, 2011.
15. Aggarwal, K. and A. Garg, "A S-shaped patch antenna for X-band wireless/microwave applications," *International Journal of Computing and Corporate Research*, Vol. 2, No. 2, 14, 2012.
16. Harrabi, A., T. Razban, Y. Mahe, L. Osman, and A. Gharsallah, "Wideband patch antenna for x-band applications," *PIERS Proceedings*, Stockholm, Sweden, Aug. 12–15, 2013.
17. Frezza, F., L. Pajewski, E. Piuzzi, C. Ponti, and G. Schettini, "Radiation-enhancement properties of an X-band Woodpile EBG and its application to a planar antenna," *International Journal of Antennas and Propagation*, Vol. 2014, Article ID 729187, 15 pages, 2014.
18. Kothapudi, V. K. and V. Kumar, "A single layer s/x-band series-fed shared aperture antenna for SAR applications," *Progress In Electromagnetics Research C*, Vol. 76, 207–219, 2017.
19. Kothapudi, V. K. and V. Kumar, "Compact 1×2 and 2×2 dual polarized series-fed antenna array for X-band airborne synthetic aperture radar applications," *Journal of Electromagnetic Engineering and Science*, Vol. 18, No. 2, 117–128, 2018.
20. Xu, H.-X., G.-M. Wang, Y.-Y. Lv, M.-Q. Qi, X. Gao, S. Ge, A. Hasnain, and M. N. Taib, "Multifrequency monopole antennas by loading metamaterial transmission lines with dual-shunt branch circuit," *Progress In Electromagnetics Research*, Vol. 137, 703–725, 2013.
21. Liu, J., Y. Cheng, Y. Nie, and R. Gong, "Metamaterial extends microstrip antenna," *Microwaves & Rf.*, Vol. 52, No. 12, 69–73, 2013.
22. Rogers Corporation, Available at: www.rogerscorp.com.
23. Computer simulation technology version, Wellesley Hills, MA, 2016, Available at: www.cst.com.